Proc. of TMS Symp. on Advances in Twinning, Feb. 28-Mar. 4, 1999, San Diego, CA (Submitted)

MICROMECHANISMS OF TWIN NUCLEATION IN TiAl: EFFECTS OF NEUTRON IRRADIATION

M. H. Yoo and A. Hishinuma*

Metals and Ceramics Division, Oak Ridge National Laboratory
Oak Ridge, TN 37831-6115, USA
*Materials Science and Engineering, Japan Atomic Energy Research Institute
Tokai-Mura, Ibaraki-Ken 319-1195, Japan

Abstract

The so-called radiation-induced ductility (RID) reported in neutron-irradiated two-phase Ti-47at%Al alloys is attributed to the formation of effective twin embryos in the presence of interstitial-type Frank loops in γ-TiAl and the subsequent nucleation and growth of microtwins during post-irradiation tensile deformation. The stability of large faulted Frank loops is explained in terms of the repulsive interaction between Shockley and Frank partials. Interaction of only six ordinary slip dislocations with a Frank loop can facilitate a pole mechanism for twin formation to work. The relative ease of heterogeneous twin nucleation is the reason for the RID and the lack of changes in yield strength and work hardening.

Introduction

The crystallography of deformation twinning in γ-TiAl of the $L1_0$ structure was determined first by Shechtman et al. [1] to be {111)<112]. The mixed-bracket notations are used here to indicate that the first two indices are not equivalent to the third in the face-centered tetragonal crystal structure. During the past decade, as research and development activities on TiAl-base alloys as high-temperature structural materials have intensified, our effort to understand the mechanistic role of deformation twinning, the so-called true-twinning, in mechanical behavior of these alloys has also increased [2-4]. It is now well established in the case of two-phase TiAl-Ti_3Al alloys that lamellar interfaces and grain boundaries are the preferred sites for twin nucleation in γ-TiAl, as summarized in the recent reviews [5-8]. In contrast, the possible role of point defects and defect clusters in the formation of deformation twins in γ-TiAl has been discussed only very recently [9-11].

DISCLAIMER

intrinsic stacking fault (ISF) energy, e.g., 15 mJ/m^2 for 304 SS [15], and TiAl has relatively low superlattice intrinsic and extrinsic stacking fault (SISF and SESF) energies, 90 and 80 mJ/m^2, and twin boundary energy, 60 mJ/m^2, compared to the antiphase-boundary (APB) energy of 560 mJ/m^2 [7], and (c) defect clusters formed by irradiation are primarily of interstitial-type Frank loops. On the other hand, the observed effects of irradiation on deformation twinning are markedly different between these two alloys.

Firstly, the number density of deformation twins in γ-TiAl grains is increased after irradiation and deformation at elevated temperature (873 K), whereas in the irradiated stainless steels, twinning is the predominant deformation mode at room temperature [15,16]. Secondly, no unfaulted Frank loops were observed in the irradiated microstructure of γ-TiAl, whereas unfaulting of Frank loops is common in irradiated stainless steels. Thirdly, no appreciable change in yielding and work-hardening behavior was observed in conjunction with the marked increase in the fracture strain [9], in contrast to the increase in yield strength and reduction in ductility usually observed in irradiated stainless steels. The present study develops a mechanistic understanding of these unique microstructural results and provides micromechanisms to explain the RID phenomenon in TiAl.

Stability of Frank Loops

The dominant point defect types in off-stoichiometric TiAl are substitutional antisite defects on both sublattices, i.e., there are no constitutional vacancies [7]. To understand the mobility of radiation-induced defects in Al-rich TiAl, Sattonnay et al. [17] performed isochronal annealing and electrical resistivity measurements after low temperature electron irradiation. Their results indicate that at 81 K (stage I) recovery by close-pair recombination is followed by self-interstitial migration, and at 444-504 K (stage III) migration and elimination of vacancies begin. This stage III is much higher than the 250 K temperature estimated from positron life-time measurements after electron irradiation by Shirai and Yamaguchi [18]. In any case, the predominance of interstitial-type loops on {111} planes in γ grains of Ti-47%Al alloy observed by TEM after electron irradiation at 573-773 K [12] is consistent with the results of electrical resistivity and positron life-time spectroscopy mentioned above.

The typical defect clusters in the specimens neutron-irradiated at 873 K to 0.05 displacement-per-atom (dpa) are shown in Fig. 1. These clusters lie on {111} planes with stacking fault fringes, and can be identified as faulted Frank loops with Burgers vector of $\langle 111\rangle/3$. The average loop diameter is about 300 nm, much larger than the foil thickness of about 150 nm, so that some of the loops are intersected by foil surfaces. Four types of {111} loop habit planes are observed, and their shapes are not circular, but elongated along the <110] directions. During irradiation, the anisotropic growth of the loops can be explained by the preferential interstitial migration on the {001) planes [19]. After the irradiation, these loops will tend to shrink by absorbing thermal vacancies. Figure 2 shows the line tension of a Frank loop as a function of the angle, θ, for the dislocation-line direction measured from the $[11\bar{2}]$ direction. The anisotropic elasticity calculations were made by using the elastic constants of Ti-56%Al [20]. The line tension at θ = 0°, perpendicular to the $[11\bar{2}]$ direction, is higher than that at θ = 90°, perpendicular to the $[\bar{1}10]$ direction, by 12-17% at 298-723 K and 43% at 1273 K. This means that the loop

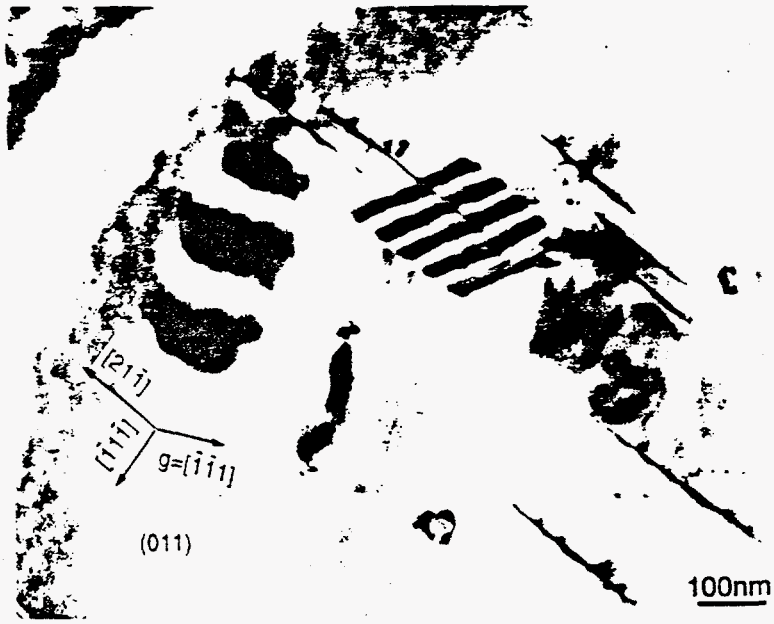

Figure 1: Faulted Frank loops of interstitial-type observed in Ti-47%Al alloy after neutron irradiation at 873 K to 1 x 10^{24} n/m^2 (E > 1 MeV) in JRR-2.

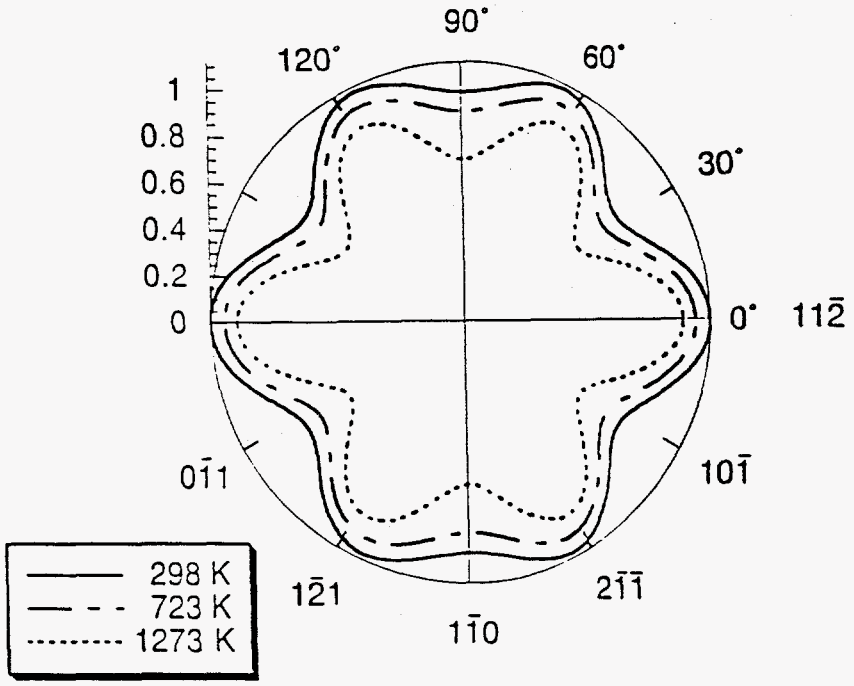

Figure 2: Anisotropic elastic line tension for a Frank loop with Burgers vector of [111]/3 at 298, 723, and 1273 K, in units of 10^{-2} GPa, calculated by using the elastic constants of Ti-56%Al [20].

will be elongated further along the [$\bar{1}$10] direction because it tends to shrink more efficiently in the [11$\bar{2}$] direction due to the relatively high line tension.

There are three different atomic sites into which an extra plane of self-interstitial Ti and Al atoms can be inserted to form an interstitial-type Frank loop, one forming SESF and the other two forming complex stacking fault (CSF). Thus, two distinctly different faults can be created, which may be called true-twin type and pseudo-twin type [21,22] or "APB type" [12], respectively. By making a circular loop approximation, the critical radius of a Frank loop, R_c, at which spontaneous unfaulting can occur by nucleation of a Shockley partial loop is given by [23]

$$\frac{R_c}{ln(R_c / r_o)} = \frac{\mu a^2 (2-\nu)}{24\pi(1-\nu)\gamma} \quad , \tag{1}$$

where r_0 is the core cut-off radius, a the lattice parameter, μ the shear modulus, ν Poisson's ratio, and γ the fault energy. The results for two fcc metals of low and high ISF energies (Cu and Al) and for 316 SS and TiAl are obtained by using the tabulated data of the elastic properties and fault energies [7,24], and they are listed in Table I. In TiAl, Eq. (1) is applicable only to the first two cases of (a) vacancy loops with SISF and (b) interstitial loops with SESF in Table I, as illustrated in Fig. 3.

Table I. Critical Radius of Frank Loops for Unfaulting

Material	(nm) a	(GPa) μ	ν	(mJ/m^2) γ	(nm) $R_c / \ell n\left(\frac{R_c}{r_o}\right)$
Cu	0.362	54.6	0.32	73	3.21
Al	0.405	26.5	0.35	200	0.73
316 SS	0.358	76.8	0.29	40	7.86
TiAl(a)	0.399	70.0	0.26	90	3.86
TiAl(b)				80	4.34
TiAl(c)				410	0.85

Electron-irradiated Cu at 473 K and Al at 423 K showed interstitial Frank loops with an average diameter of about 100 nm [26]. In the former, all the loops appeared faulted, suggesting that $R_c > 100$ nm. In quenched-in Al, the average diameter of vacancy loops was in the range of 25 - 100 nm [27,28], depending on the quenching temperature. In this case, some of the loops were unfaulted, i.e., $R_c \approx 25$ - 100 nm. Direct evidence for the spontaneous unfaulting of interstitial Frank loops was reported in a Fe-Cr-Ni alloy, the model ternary alloy for austenitic stainless steel, after dual-ion (Ni-He) irradiation [29]. This gives the average loop diameter as $R_c \approx 200$ nm. All together, if we assume that the ESF and SF energies are equal, these TEM data are consistent with the critical radii

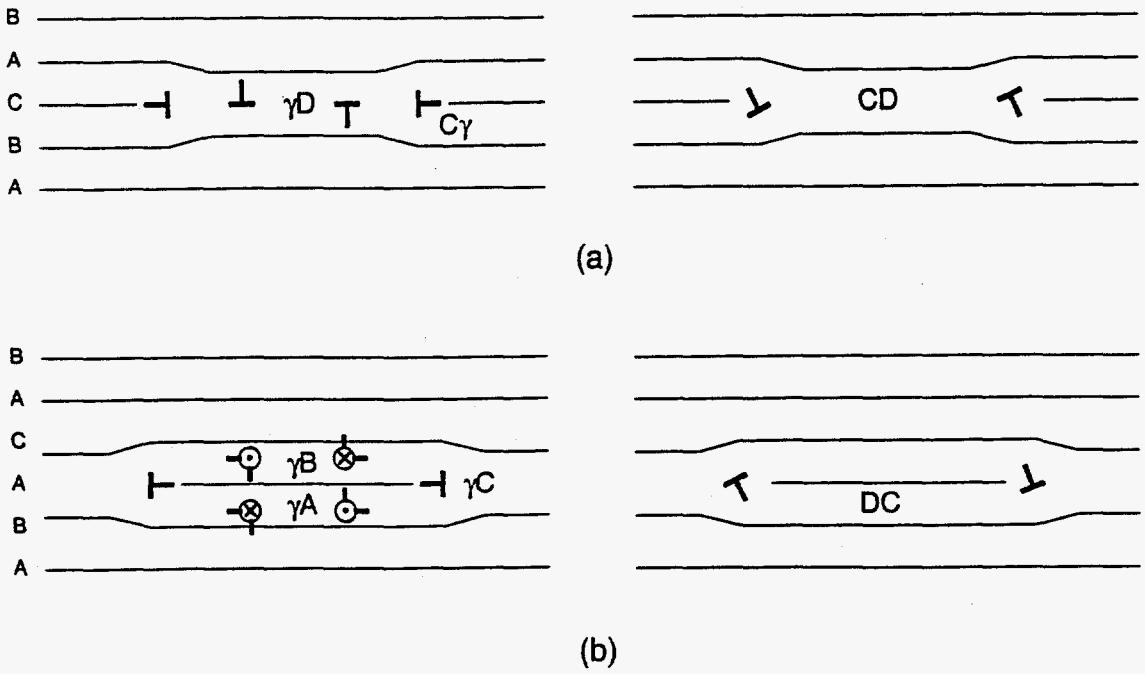

Figure 3: Unfaulting of Frank loops of (a) vacancy type with SISF and (b) interstitial type with SESF by nucleation of a Shockley and a composite-Shockley [25] loops, respectively. $[112]/6 + [11\bar{1}]/3 = [110]/2$ on $(11\bar{1})$ is equivalent to $\mathbf{D\gamma + \gamma C = DC}$ on (c) in Thompson's notation.

estimated in Table I. According to the review on evolution of Frank loops in stainless steels [30], the loop number density drops drastically at the irradiation temperature of 623 K. In γ-TiAl electron-irradiated to 1 dpa [12], very few defect clusters were observed, < 2 x 10^{20} m^{-3}, at temperatures above 723 K. In view of the above results (Table I) and the comparable melting points of these two alloys, the relatively large faulted Frank loops (≈300 nm) observed in Ti-47%Al alloy (Fig. 1) after irradiation at 873 K is somewhat surprising. Effects of nucleation barrier and segregation may contribute also to the metastability of large size Frank loops in TiAl. Nevertheless, these loops are likely to be the SESF type since the R_c of this type is larger than that of the CSF type by a factor of more than five.

Formation of Twin Sources

While all four {111} planes are equally populated with interstitial Frank loops, only a few selective slip and twin systems will be activated in each γ-TiAl grain at the early stage of tensile deformation. Proper combinations of ordinary slip, superlattice slip, and twin systems can be selected with the aid of Fig. 4 and Table II. Two cases, [021] and $[\bar{1}11]$, are of interest because (a) in the former the Schmid factor is high, $\alpha = 0.46$, for both ordinary slip and twinning, and (b) in the latter $\alpha = 0.39$ for both superlattice slip and twinning. Also, at these two tensile orientations, the directional sense of superdislocations (Fig. 4(b)) does not depend on any specific sign convention [31]. Interactions between a Frank loop and slip dislocations are classified into two types [28,32], Type I when the slip planes are parallel to the loop plane and Type II when they are not. Because of the large

size of elongated Frank loops (Fig. 1), only Type II interactions are discussed in this paper.

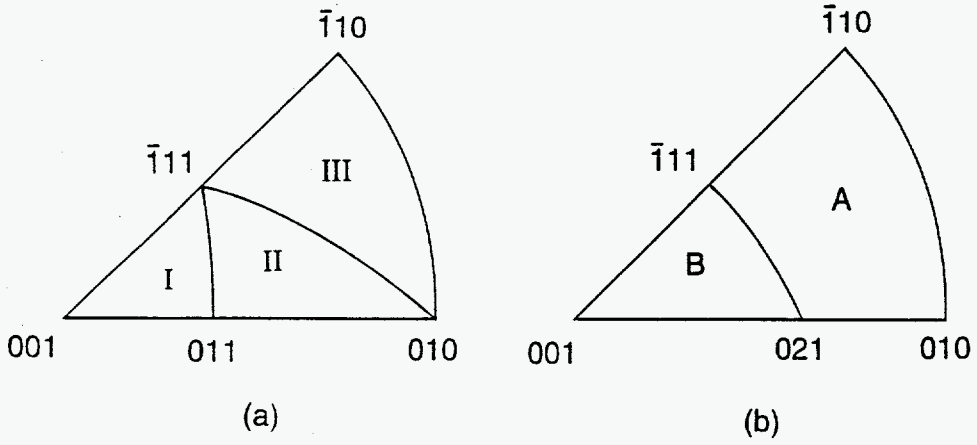

Figure 4: Stereographic projections for the uniaxial tension directions and the operative slip systems, (a) the regions I and III for superlattice slip and the region II for ordinary slip, and (b) the tension/compression asymmetry and the direction of motion of <101] superdislocations.

Ordinary Slip

When an ordinary $(1\bar{1}1)[110]/2$ slip dislocation, (a) **DC** in Thompson's notation, with the Schmid factor of $\alpha = 0.46$ interacts with a Frank loop on the $(11\bar{1})$ or (c) plane, the reaction occurs according to

$$[11\bar{1}]/3 + [112]/6 = [110]/2 \quad \text{or} \quad \gamma\mathbf{C} + \mathbf{D}\gamma = \mathbf{DC} \quad , \qquad (2)$$

and after intersection by the slip dislocation is completed, the sheared loop may appear as illustrated in Fig. 5(a). The originally elliptic loop, with the major axis along the $[\bar{1}10]$ direction (**AB** in Fig. 5), is now sheared into two connected by a rectangular loop (unfaulted) bounded by a long dipole of **D**γ/γ**D** and two **DC/CD** jogs. The **D**γ/γ**D** dipole is separated only by a short atomic distance of magnitude, DC = $a/\sqrt{2}$, which can increase as more slip dislocations intersect the loop at the same plane. When several dislocations of the same $(1\bar{1}1)[110]/2$ slip system, moving in the parallel but adjacent planes, intersect at different parts of the Frank loop, the twin nucleation process suggested by Song et al. [32] may occur with the help of thermal activation or a local stress concentration under the applied stress ($\alpha = 0.46$).

Superlattice Slip

A superdislocation of the $(1\bar{1}1)[10\bar{1}]$ slip system ($\alpha = 0.39$) may be dissociated into three partials according to [7]:

$$[10\bar{1}] \longrightarrow [1\bar{1}\bar{2}]/6 + \text{SISF} + [21\bar{1}]/6 + \text{APB} + [10\bar{1}]/2 \qquad (3a)$$

or

Table II. Schmid Factors for Possible Slip/Twin Systems
($\alpha > 0$ Under Tension, c/a = 1)

Slip/Twin Systems	Tensile Loading Axes				
	[001]	[021]	[$\bar{1}$11]	[010]	[$\bar{1}$10]
(111) [1$\bar{1}$0]	0	0	0.385	-0.289	0
(11$\bar{1}$) [1$\bar{1}$0]	0	0.462	0.385	0.289	0
(1$\bar{1}\bar{1}$) [110]	0	0	0	-0.289	0.471
(1$\bar{1}$1) [110]	0	0.462	0	0.289	0.471
(111) [01$\bar{1}$]	-0.289	0.173	0	0.289	0
(1$\bar{1}\bar{1}$) [01$\bar{1}$]	-0.289	0.173	0	0.289	0.236
(1$\bar{1}\bar{1}$) [10$\bar{1}$]	0.289	-0.173	-0.385	0	0
(1$\bar{1}\bar{1}$) [10$\bar{1}$]	0.289	0.289	0.385	0	-0.236
(1$\bar{1}\bar{1}$) [011]	-0.289	0.173	0.385	0.289	0
(1$\bar{1}\bar{1}$) [011]	-0.289	0.173	-0.385	0.289	-0.236
(1$\bar{1}\bar{1}$) [101]	0.289	0.289	0	0	0
(1$\bar{1}\bar{1}$) [101]	0.289	-0.173	0	0	0.236
(111) [11$\bar{2}$]	0	0	-0.385	0.289	0
(11$\bar{1}$) [112]	0	0.462	0.385	0.289	0
(1$\bar{1}\bar{1}$) [1$\bar{1}$2]	0	0	0	0.289	0
($\bar{1}$1$\bar{1}$) [$\bar{1}$12]	0	0.462	0	0.289	0

$$2\mathbf{BC} \longrightarrow \mathbf{B}\alpha + \text{SISF} + \alpha\mathbf{C} + \text{APB} + \mathbf{BC} \quad . \tag{3b}$$

When this dislocation moves to the right (when the tensile axis is in the region B in Fig. 4(b)), the leading superpartial (**BC**) will interact with the Frank loop in a similar manner as in Fig. 5(a), except that in this case the rectangular loop contains a strip of APB as shown in Fig. 5(b). This is eliminated after the whole dislocation (2**BC**) cut through the loop. On the other hand, when the leading Shockley partial (**B**α) intersects the loop (the region A in Fig. 4(b)), the sheared loop configuration is similar to Fig. 5(b) except that a strip of SISF is bounded by the long $\gamma\alpha/\alpha\gamma$ stair-rod dipole and **B**α/α**B** jogs. In either case, after the whole dislocation (2**BC**) intersects the loop, the end result will be the same. Unlike the case A of ordinary dislocations, however, the partial dislocations accumulated by intersection of a slip-band with the loop are $\mathbf{B}\gamma = [1\bar{2}\bar{1}]/6$ type. Consequently, even if a twin nucleus is formed, this will be of pseudo-twin type.

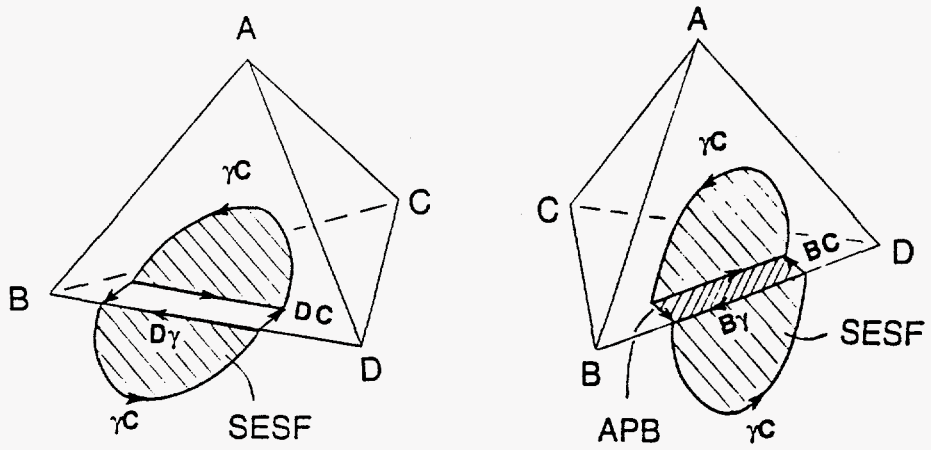

$\gamma C + D\gamma = DC$ (a)

$\gamma C + B\gamma = BC$ (b)

Figure 5: Intersections of a Frank loop (γ**C**) by (a) an ordinary slip dislocation (**DC**) and (b) a superpartial dislocation (**BC**). Short jogs and a long Shockley dipole are formed on the Frank loop. The narrow rectangular strip is unfaulted in (a) and contains APB in (b).

Twin Nucleation and Growth

The critical stages of twin nucleation, as depicted in Figs. 6 and 7, can be discussed on the basis of our earlier work [10]. The critical shear stress, τ_2, for **D**γ Shockley partials to expand beyond the semicircle with the minor radius, a_F, of a Frank loop, Fig. 6(b), can be estimated by

$$n\tau_2 = \frac{\gamma_E}{b_t} + (K + K'')\frac{b_t}{2\pi} ln\left(\frac{a_F}{r_o}\right), \qquad (4)$$

where b_t is the magnitude of **D**γ, K + K" is the energy factor of a **D**γ partial and its second derivative with respect to θ, and n is the local stress concentration factor. This equation differs from Eq. (4) of Ref. [10] in that γ_E is the SESF energy and the third term for Shockley-Frank interaction is neglected. As compared to the first term in Eq. (4), 488 MPa, the second term becomes relatively small, e.g., 60 MPa when a_F = 240 nm. This means that $n\tau_2 = n\alpha\sigma_y$ = 548 MPa, and n = 3.8 since the yield stress is about σ_y = 450 MPa [9] and α = 0.46.

The critical stress, τ_1, to separate the **D**γ partial from the γ**D** counterpart of a dipole (Fig. 6(a)) is estimated, by considering the screw components of **D**γ/γ**D** (30°-mixed dislocations), to be $n\tau_1 = \mu/25$. By setting $\tau_1 = \tau_2$ and using μ = 70 GPa (Table I), we find that n = 5.1. This means that local stress concentration at a jogged Frank loop by six or more **DC** dislocations of the ordinary slip system is sufficient to overcome both the critical stresses for the first-half of a revolution by twinning partials around the two poles.

The mechanical driving force to expand the Frank loop is very small, $\sigma_F = \beta\sigma$, where σ_F is the resolved normal stress on the loop plane, σ is the applied tensile stress, and β = 0.07

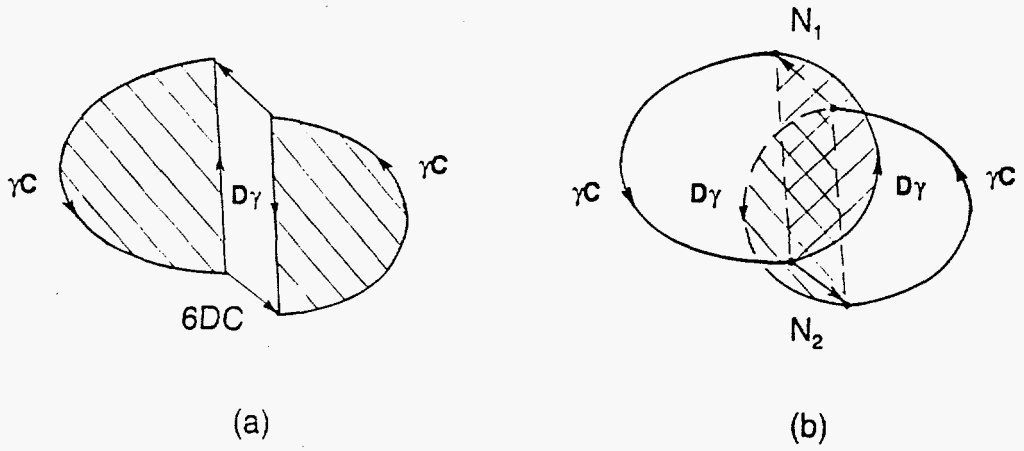

Figure 6: Early stage of twin formation by expansion of two Shockley partials (**D**γ) anchored around two poles (N_1 and N_2) separated by the length of the minor diameter, $2a_0$. (a) Two parts of a Frank loop with SESF (hatched areas) jogged by 6 **DC** dislocations, and (b) the critical stage of Shockley's expansion (hatched areas) for the first revolution.

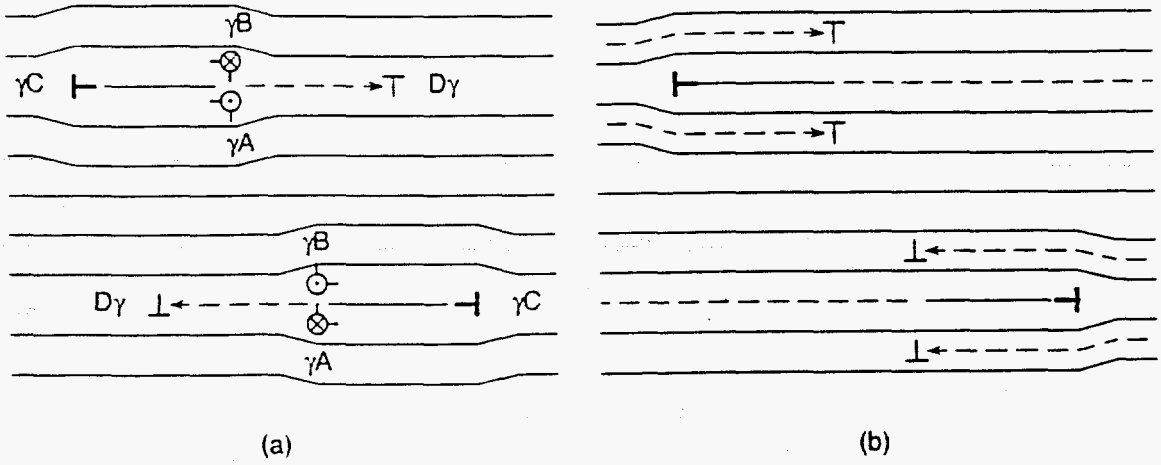

Figure 7: Cross-sectional view of the motion of Shockley partials. (a) The jogged Frank loop (γ**C**) corresponding to Fig. 6(a) is shown with the synchro-Shockley partials (γ**A** and γ**B**), and the critical stage of Fig. 6(b) is shown by the Shockley partial (**D**γ), and (b) the motion of the Shockley partials at the transient stage after a full revolution is indicated by dashed arrows.

for the [021] orientation. The chemical stress to shrink the Frank loop by absorbing vacancies is expected to be much higher at 873 K. The geometrical difficulty of the pole mechanism for twin nucleation in the fcc structure, after one full revolution, was circumvented by introducing unit jogs on **DC** pole dislocations after recombination of **D**γ + γ**C** → **DC** [33]. In the present case, the expanding **D**γ partials encounter the segments of γ**C** loops at three-quarters of a full revolution, where the recombination and formation of a unit jog can take place. Such a jog formation is relatively easy in the present case of neutron-irradiated TiAl when there are nonequilibrium Frank loops acting as heterogeneous sites for twin nucleation.

As compared to the previous case of twin nucleation which evolved from a SISF loop [10], growth kinetics of a twin nucleus is expected to be slower because the motion of a true-twinning $D\gamma$ partial trailing SESF may occur by the synchroshear process of a composite Shockley [25], i.e., γA and γB pseudo-twinning partials in the two adjacent $(11\bar{1})$ planes as shown in Fig. 3(b),

$$[112]/6 = [2\bar{1}1]/6 + [\bar{1}21]/6 \text{ or } D\gamma = \gamma A + \gamma B \quad . \qquad (5)$$

In terms of the ease of gliding parameters, which is the exponential factor for Peierls stress, the mobility of synchro-Shockley partials (γA and γB) is lower than that of a Shockley partial ($D\gamma$) by 17% and 8% for the edge and screw components, respectively [34]. Therefore, the growth kinetics of deformation twins by extending SESF is believed to be slower than that by extending SISF. As was discussed earlier in the case of the asymmetric motion of a [112]/2 superdislocation [7], if the expanding $D\gamma$ partial is to trail a SISF (a monolayer twin) instead of a SESF (a two-layer twin), then the twin growth kinetics will be the same as when no precursors (SESFs) for twin formation exist [10]. Fig. 7(b) depicts the latter case where each $D\gamma$ Shockley trailing a SISF thickens the preexisting SESF by two atomic layers, one above and one below, after a full revolution.

Discussion

The presence of large faulted interstitial-type Frank loops observed in Ti-47%Al alloys after neutron irradiation is rationalized from the viewpoint of energetics and by comparing with the available experimental data on fcc metals and alloys. In the fcc crystals, the reaction of a [110]/2 dislocation into a Shockley-Frank partial pair, Eq. (2), is energetically indeterminate, regardless of the degree of elastic anisotropy [10]. Whereas, in the $L1_0$ structure, dissociation is favored at non-screw orientations on account of the strong out-of-plane component of the repulsive interaction between these two partials [35]. If a Shockley partial loop was to nucleate at the center of a Frank loop, Fig. 3(b), this repulsive interaction due to the non-cubic elastic anisotropy will suppress the full expansion of the Shockley loop to complete the unfaulting process. This may be the reason why unfaulting of Frank loops is more difficult in TiAl than in fcc metals and alloys. After high-voltage electron microscopy experiments on Fe-Cr-Ni single crystals, Suzuki et al. [36] concluded that unfaulting of interstitial-type Frank loops is more difficult than in a vacancy type owing to the simultaneous operation of two shear motions required for removing the SESF. Our view of the difference in mobility between a Shockley partial and synchro-Shockley partials, Eq. (5), in $L1_0$ alloys is consistent with this experimental result.

An extension has been made of the earlier work of dislocation pole mechanism [10] which was proposed to explain the experimental data of twin formation in Ti-56%Al single crystals compressed along the [001] direction at elevated temperatures (> 1000 K) [37]. In the absence of Frank loops, the formation of a super-jog on [110]/2 dislocation and the necessary stress concentration are provided by the active <101] superdislocations. In the present case of twin formation at pre-existing Frank loops of interstitial type, we find that only six or more <110]/2 ordinary dislocations are needed to form the critical jogs on a Frank loop and to raise the local internal stress to exceed the critical stresses. This result supports the original contention that the difficult stage of twin nucleation in TiAl was overcome by the Frank loops introduced by neutron irradiation [9]. The nucleation model proposed by Song et al. [32] gives essentially the same end result (their Fig. 6) as our

model in that a twin nucleus can emerge from a Frank loop as a result of the slip-loop interactions. The main difference between the two models is that while their model gives the thickness of twin nucleus limited to the number of <110]/2 dislocations that intersect the loop, our model provides a three-dimensional description of the twin nucleation and growth beyond the twin thickness of six atomic layers.

The fact that yielding and work-hardening were essentially unchanged while the tensile elongation was increased [9] cannot be readily explained by the proposed mechanism. In view of the necessary stress concentration ($n > 6$), which is rather low as compared to the earlier case [10], the hardening due to the slip-loop interactions in TiAl may not be as large as one might have anticipated. Since the tensile behavior was recorded in two-phase Ti-47%Al polycrystalline alloys [9], possible indirect role of irradiation effects on α_2 phase, such as enhanced deformation and/or localized disordering at interfaces, may deserve some further research in the future.

Summary

The stability of interstitial-type Frank loops in γ-TiAl created by neutron irradiation and the subsequent heterogeneous nucleation and growth of deformation twins were analyzed from the energetic and kinetic points of view. The main results of this analysis are:

(1) The elongated shape of interstitial Frank loops along the <110] direction is explained not only by the preferential interstitial migration on the {001) plane during irradiation, but also by the preferential shrinkage of the loops along the <112] direction after the irradiation.

(2) The stability of faulted Frank loops observed in TiAl, in contrast to the frequent unfaulting of Frank loops reported in fcc metals and alloys, is consistent with the repulsive elastic interaction between Shockley and Frank partials and the synchroshear motion of a composite Shockley partial in the case of interstitial type.

(3) When a Frank loop is intersected by six or more ordinary <110]/2 slip dislocations, the resulting Shockley dipole can be separated, and each Shockley partial can expand and spiral around the two poles to create a twin nucleus. Growth kinetics of the twin nucleus depends on the mobility of synchro-Shockley partials which is lower than that of a Shockley partial.

(4) The relative ease of twin nucleation as a result of the interaction between a Frank loop and slip dislocations is the reason for the RID, and the predicted result of a rather low stress concentration resulting from only six ordinary dislocations is consistent with the lack of changes in yield strength and work-hardening reported in Ti-47%Al alloys.

Acknowledgment

The authors would like to thank E. P. George, S. J. Zinkle, T. Sawai, and P. J. Maziasz for helpful discussions and J. F. McKinney for preparing the manuscript. This research was sponsored by the Division of Materials Sciences, Office of Basic Energy Sciences,

U.S. Department of Energy under contract number DE-AC05-96OR22464 with Lockheed Martin Energy Research Corp.

References

1. D. Shechtman, M. J. Blackburn, and H. A. Lipsitt, "The Plastic Deformation of TiAl," Metall. Trans. 5 (1975), 1373-1381.

2. M. H. Yoo and M. Wuttig, ed., Twinning in Advanced Materials, TMS, Symp. Proc. (Warrendale, PA.: TMS, 1994).

3. Y.-W. Kim, R. Wagner, and M. Yamaguchi, ed., Gamma Titanium Aluminides, TMS Symp. Proc. (Warrendale, PA.: TMS, 1996).

4. K. S. Chan, V. K. Vasudevan, and Y.-W. Kim, ch., Fundamentals of Titanium Aluminides, TMS Symp., (a collection of papers in Metall. Mater. Trans. A29 (1998), 1).

5. M. Yamaguchi and Y. Umakoshi, "The Deformation Behavior of Intermetallic Superlattice Compounds," Prog. Mater. Sci. 34 (1990), 1-148.

6. J. W. Christian and S. Mahajan, "Deformation Twinning," Prog. Mater. Sci. 39 (1995), 1-157.

7. M. H. Yoo and C. L. Fu, "Physical Constants, Deformation Twinning, and Microcracking of Titanium Aluminides," Metall. Mater. Trans. 29A (1998), 49-63.

8. F. Appel and R. Wagner, "Microstructure and Deformation of Two-Phase γ-Titanium Aluminides," Mater. Sci. Eng. R22 (1998), 187-268.

9. A. Hishinuma, K. Fukai, T. Sawai, and K. Nakata, "Ductilization of TiAl Intermetallic Alloys by Neutron-Irradiation," Intermetallics 4 (1996), 179-184.

10. M. H. Yoo, "On the Dislocation Pole Mechanism for Twinning in TiAl crystals," Phil. Mag. Lett. 76 (1997), 259-268.

11. M. H. Yoo and A. Hishinuma, "Deformation Twinning in TiAl: Effects of Defect Clustering," Metals Mater. 3 (1997) 65-74.

12. A. Hishinuma, "Radiation Damage of TiAl Intermetallic Alloys," J. Nucl. Mater. 239 (1996), 267-272.

13. J. L. Brimhall, J. I. Cole, and S. M. Bruemmer, "Deformation Microstructures in Ion-Irradiated Stainless Steel," Scr. Metall. Mater. 30 (1994), 1473-1478.

14. J. I. Cole and S. M. Bruemmer, "Post-Irradiation Deformation Characteristics of Heavy-Ion Irradiated 304L SS," J. Nucl. Mater. 225 (1995), 53-58.

15. J. L. Brimhall, J. I. Cole, J. S. Vetrano and S. M. Bruemmer, "Temperature and Strain-Rate Effects of Deformation Mechanisms in Irradiated Stainless Steel," Microstructure of Irradiated Materials, ed. I. M. Robertson, L. E. Rehn, S. J. Zinkle, and W. J. Phythian, MRS Symp. Proc. Vol. 373 (Pittsburgh, PA: The Materials Research Society, 1995), 177-182.

16. R. D. Carter, M. Atzmon, G. S. Was, and S. M. Bruemmer, "Deformation Mechanisms in a Proton-Irradiated Austenitic Stainless Steel," *ibid.*, 171-176.

17. G. Sattonnay, F. Ma, C. Dimitrov, and O. Dimitrov, "Radiation-Induced Defects in Electron-Irradiated γ-TiAl Compounds: the Effect of Composition," J. Phys.: Condens. Matter **9** (1997), 5527-5541.

18. Y. Shirai and M. Yamaguchi, "Studies of Vacancies and Dislocations in TiAl by Positron Annihilation," Mater. Sci. Eng. A152 (1993), 173-181.

19. K. Nakata, K. Fukai, A. Hishinuma, K. Ameyama, and M. Tokizane, "Dislocation Loop and Cavity Formation under He-Ion Irradiation in a Ti-Rich TiAl Intermetallic Compound," J. Nucl. Mater. 202 (1993), 39-46.

20. Y. He, R. B. Schwarz, T. Darling, M. Hundley, S. H. Whang, and Z. M. Wang, "Elastic Constants and Thermal Expansion of Single Crystal γ–TiAl from 300 to 750 K," Mater. Sci. Eng. A239-240 (1997),157-163.

21. J. W. Christian and D. E. Laughlan, "The Deformation Twinning of Superlattice Structures Derived from Disordered b.c.c. or f.c.c. Solid Solutions," Acta Metall. 36 (1988), 1617-1642.

22. M. H. Yoo, C. L. Fu, and J. K. Lee, "Deformation Twinning in Metals and Ordered Intermetallics - Ti and Ti-Aluminides," J. Phys. III, 1 (1991) 1065-1084.

23. F.R.N. Nabarro, Theory of Dislocations (Oxford: Clarendon Press, 1967), 360-364.

24. J. P. Hirth and J. Lothe, Theory of Dislocations (New York: McGraw Hill, 1968), 761-764.

25. G. Hug and P. Veyssiére, "TEM Observation of Dislocation Substructures and Micro-Twins in Manganese-Doped TiAl," Electron Microscopy in Plasticity and Fracture Research of Materials, ed. U, Messerschmidt, F. Appel, J. Heidenrich and V. Schmidt (Berlin: Akademie-Verlag, 1989), 451-458.

26. M. Kiritani and H. Takata, "Dynamic Studies of Defect Mobility using High Voltage Electron Microscopy," J. Nucl. Mater. 69-70 (1978), 277-309.

27. R.M.J. Cotterill, "Vacancy Clusters in Pure and Impure f.c.c. Metals," Lattice Defects in Quenched Metals, ed. R.M.J. Cotterill, M. Doyama, J. J. Jackson, and M. Meshii (New York: Academic Press, 1965), 97-162.

28. J. L. Strudel and J. Washburn, "Direct Observations of Interactions between Imperfect Loops and Moving Dislocations in Aluminium," Phil. Mag. 9 (1964), 491-506.

29. E. H. Lee and L. K. Mansur, "Evidence for a Mechanism of Swelling Variation with Composition in Irradiated Fe-Cr-Ni Alloys," Phil. Mag. A 52 (1985), 493-508.

30. S. J. Zinkle, P. J. Maziasz, and R. E. Stoller, "Dose Dependence of the Microstructural Evolution in Neutron-Irradiated Austenitic Stainless Steel," J. Nucl. Mater. 206 (1993), 266-286.

31. M. H. Yoo and M. Yamaguchi, "Interfacial Structures and Mechanical Properties of Titanium Aluminides," Microstructure and Properties of Materials, Vol. 2, ed. J.C.M. Li (Singapore, World Scientific, 1999), to be published.

32. S. G. Song, J. L. Cole, and S. M. Bruemmer, "Formation of Partial Dislocations during Intersection of Glide Dislocations with Frank Loops in f.c.c. Lattices," Acta Mater. 45 (1997), 501-511.

33. J. A. Venables, "Deformation Twinning in Face-Centered Cubic Metals," Phil. Mag. 6 (1961), 379-396.

34. M. H. Yoo, C. L. Fu, and J. K. Lee, "Elastic Properties of Twin Dislocations in Titanium Aluminides," Twinning in Advanced Materials, ed. M. H. Yoo and M. Wuttig (Warrendale, PA.: TMS, 1994), 97-106.

35. M. H. Yoo, "Dislocation Mechanisms for Deformation Twinning in the $L1_0$ Structure," Scr. Mater. 39 (1998), 569-575. 1998.

36. M. Suzuki, A. Sato, T. Mori, J. Nagakawa, N. Yamamoto, and H. Shiraishi, "*In Situ* Deformation and Unfaulting of Interstitial Loops in Proton-Irradiated Steels," Phil. Mag. A 65 (1992), 1309-1326.

37. H. Inui. M. Matsumuro, D.-H. Wu, and M. Yamaguchi, "Temperature Dependence of Yield Stress, Deformation Mode and Deformation Structure in Single Crystals of TiAl (Ti-56at.%Al)," Phil. Mag. A 75 (1997), 395-423.